Journal of Metals, Materials and Minerals, Vol. 33, No. 1, pp. 21-26, 2023

Examination of the adhesion of the scale formed on hot-rolled steel with different silicon content using a tensile test

Seksan SINGTHANU[1], Prayoon SURIN[1], Thanasak NILSONTHI[2], and Manop PIPATHATTAKUL[1,*]

[1] *Faculty of Engineering, Pathumwan Institute of Technology, 833 Rama1 Road, Wang Mai, Pathumwan, Bangkok, 10330, Thailand*
[2] *High Temperature Corrosion Research Centre and Department of Materials and Production Technology Engineering, Faculty of Engineering, King Mongkut's University of Technology North Bangkok, 1518, Pracharat 1 Road, Wongsawang, Bangsue, Bangkok, 10800, Thailand*

***Corresponding author e-mail:** manop.mt@gmail.com

Received date:
29 December 2022
Revised date
10 March 2023
Accepted date:
13 March 2023

Keywords:
Tensile test;
Oxide scale;
Scale adhesion;
Hot-rolled steel

Abstract

In the hot-rolling process, steel was subjected to high temperatures which results in the formation of an oxide layer called scale. The oxide scale can be affected to the surface characteristic of the hot-rolled steel product. The scale must be completely removed from the surface of the steel before further processing. This research aimed to examine the adhesion behavior of scale on hot-rolled steel with different silicon contents (0.01, 0.12, 0.18, and 0.29 wt%) using a tensile testing machine with an observation setup. The results showed that the scale thickness decreased with increasing silicon content in the range of 9 µm to 12 µm. The scales were composed of hematite and magnetite. The results of the tensile test showed that the strain initiating the first spallation and the mechanical adhesion energy tend to increase with increasing silicon content. However, it decreased by 0.29 wt% Si hot-rolled steel. This result indicates that scale was difficult to remove after the hot rolling process for higher Si-containing steel.

1. Introduction

An oxide scale, also known as an oxide layer, forms on the steel surface during the hot rolling process. This scale should be removed before the next process, e.g. cold rolling process. Due to the scale significantly impacts to the surface quality of the final products. The mechanical properties of hot-rolled steel are improved by alloying element, e.g. Si, Cu, Ni, Sn, S, P, etc. Steel is alloyed with various elements to improve its strength, ductility, electrical conductivity, corrosion resistance, and other properties. During the hot rolling process, the scale is usually removed via high-pressure water (150 bar to 160 bar) [1-5]. Iron-oxide scale is mainly produced during the hot-rolled steel surface exposed to air atmosphere and always formed on the steel surface during the process until the hot-rolled coil product [6-14]. The characteristic of the oxide scale depends on the alloying element [15-19], hot rolling temperature [20-24], atmosphere, rolling speed, reduction per pass, etc. The presence of Si in the hot-rolled steel considerably impacted the formation and adhesion of the thermal oxide scale during the hot-rolling process. The de-scaling process is affected by this scale. The picklability of the oxide scale on steel substrate assess via an immersion test [25,26]. The scale adhesion has been measured by various techniques such as an indentation test [27,28], the tensile test [29-33]. This study aimed to assess the effect of Si content in the hot-rolled steel on the mechanical adhesion of the oxide scale by using a tensile testing machine with an observation set (CCD camera).

2. Experimental

2.1 Materials

Table 1 presents the chemical composition of the studied steel. The as-received hot-rolled steel is different in Si content as 0.010, 0.125, 0.188, and 0.292 wt% with the other alloying elements tend to be similar. The steel is obtained from Sahaviriya Steel Industries Public Company Limited (SSI) as strips with a thickness of 3.2 mm. The hot-rolling process produced the hot-rolled steel strips with a finishing temperature of 860°C and a coiling temperature in range of 630°C to 650°C.

Table 1. Chemical composition of the hot-rolled steel.

Hot-rolled steel	Composition (wt%)						
	C	Si	Cu	Mn	P	S	Fe
0.013 wt% Si	0.170	0.013	0.009	1.047	0.020	0.007	Balance
0.125 wt% Si	0.135	0.125	0.011	0.900	0.015	0.003	Balance
0.188 wt% Si	0.120	0.188	0.031	1.395	0.022	0.022	Balance
0.293 wt% Si	0.164	0.293	0.022	1.163	0.023	0.010	Balance

2.2 Characterization

The oxide scale morphology is observed by using a scanning electron microscope (SEM, Quanta 450) with energy-dispersive X-ray spectroscopy (EDS). The oxide scale compound is analyzed by using X-ray diffraction (XRD, Smart Lab) with Cu Kα (λ = 0.15406 nm), a step size and step time of 0.02 degree/step and 0.5 second/step respectively.

2.3 Adhesion test

The tensile testing machine (Model 5566) with an observation set (CCD camera) is used to study the scale adhesion on the as-received hot-rolled steel. The tensile testing machine with a tension load of 10 kN and a strain rate of 0.04 s^{-1} are performed. A CCD camera equipped with a high-magnification lens is selected to monitor the progression of scale failure during the tensile test. The image processing software is used to evaluate the image. The tensile test sample is prepared by following the ASTM E8M standard with 2 mm of thickness via a laser cutting machine. The tensile test setup and specimen shape are shown in Figure 1.

3. Results and discussion

3.1 Oxide scale characteristic

Figure 2 shows the scale thickness of the as-received hot-rolled steel. The scale thickness was directly measured from the cross-sectional SEM image by measuring five positions. The scale thickness tends to decrease with increasing Si content in the steel. The result shows the scale thickness of 0.01 wt% Si steel was 11.30 ± 0.68 μm. The scale thickness of 0.12 wt% Si steel was 10.47 ± 0.43 μm. The scale thickness of 0.18 wt% Si steel was 10.05 ± 0.79 μm, and the scale thickness of 0.29 wt% Si steel was 9.53 ± 0.46 μm.

For 0.01 wt% Si steel, Figure 3 shows SEM image, Figure 4 shows EDS pattern at interface, and Figure 5 shows XRD pattern. The result showed that the scale thickness was 11.30 ± 0.68 μm with hematite (Fe_2O_3) and magnetite (Fe_3O_4) layers. At steel-scale interface, peaks of C, O, Fe, and Mn were observed. It can be noted that the peak of Si was not observed at interface.

For 0.12 wt% Si steel, Figure 6 shows SEM image, Figure 7 shows EDS pattern at interface, and Figure 8 shows XRD pattern. The result showed that the scale thickness was 10.47 ± 0.43 μm with hematite (Fe2O3) and magnetite (Fe3O4) layers. At steel-scale interface, peaks of C, O, Fe, Mn, and Si were observed.

For 0.18 wt% Si steel, Figure 9 shows SEM image, Figure 10 shows EDS pattern at interface, and Figure 11 shows XRD pattern. The result showed that the scale thickness was 10.05 ± 0.79 μm with hematite (Fe_2O_3) and magnetite (Fe_3O_4) layers. At steel-scale interface, peaks of C, O, Fe, Mn, and Si were observed.

For 0.29 wt% Si steel, Figure 12 shows SEM image, Figure 13 shows EDS pattern at interface, and Figure 14 shows XRD pattern. The result showed that the scale thickness was 9.53 ± 0.46 μm with hematite (Fe_2O_3) and magnetite (Fe_3O_4) layers. At steel-scale interface, peaks of C, O, Fe, Mn, and Si were observed.

From the results, the silicon content was affected to scale formation of the hot-rolled steel. The scale thickness was decreased with increasing Si content in the hot-rolled steel. This was due to the Si element can be easily oxidized at a high temperature more than the other alloying element. It affected to form silicon oxide (SiO_2) at the steel-scale interface during initial oxidation. This layer may exhibit as a barrier for Fe and O to oxidize. It was seen that the higher Si-containing steel had a lower scale thickness. Furthermore, the presence of SiO_2 barrier layer at the steel-scale interface affects 0.29 wt% Si hot-rolled steel by inducing discontinuous scale morphology.

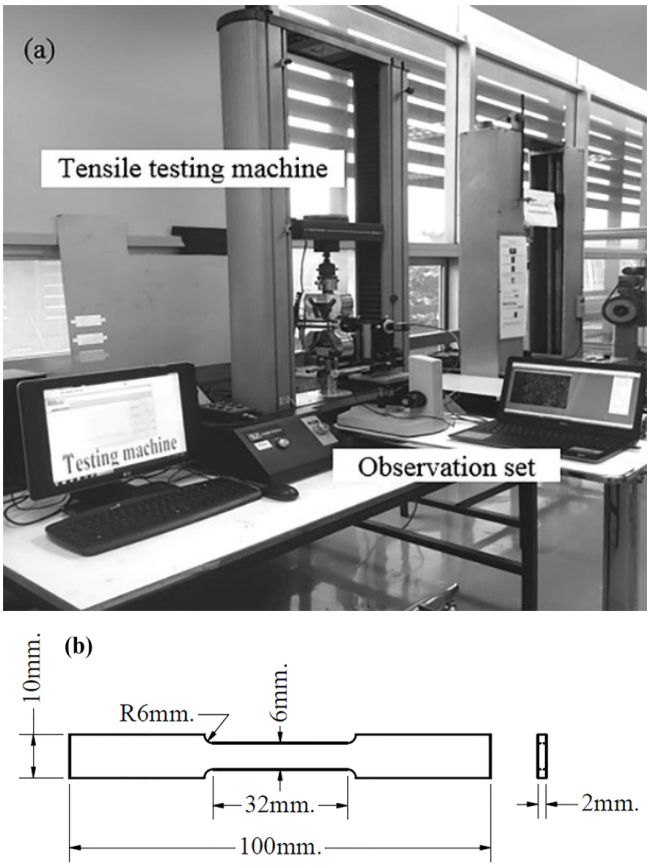

Figure 1. Tensile testing machine with an observation setup (a), and a specimen shape (b).

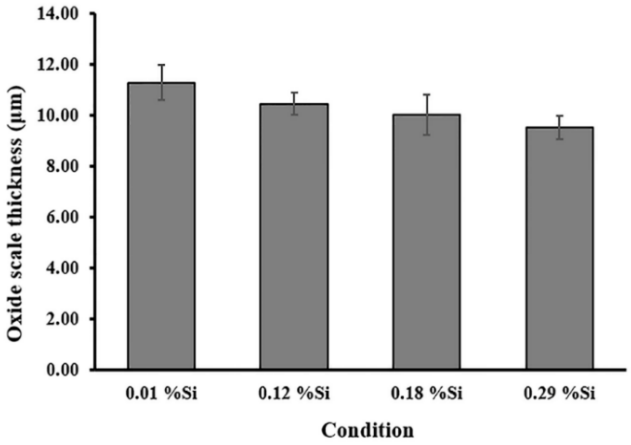

Figure 2. Oxide scale thickness of the Si-containing hot-rolled steel.

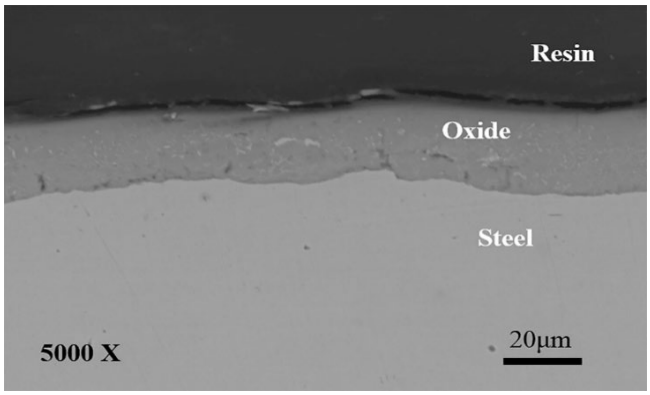

Figure 3. SEM image of 0.01 wt% Si steel.

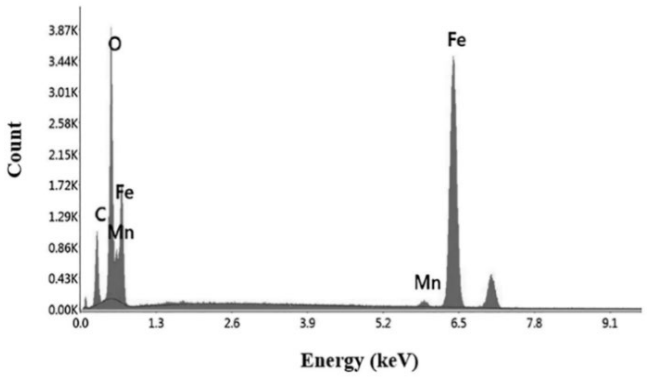

Figure 4. EDS pattern at steel-scale interface of 0.01 wt% Si steel.

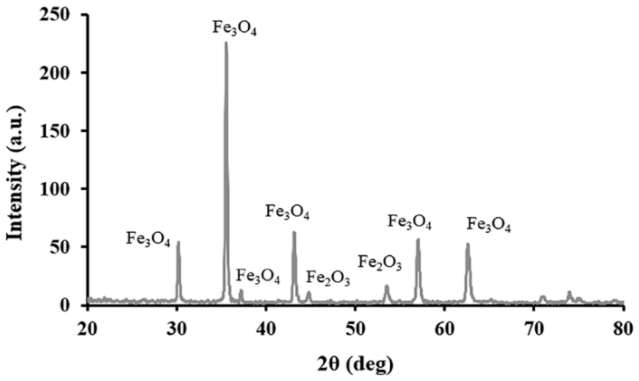

Figure 5. XRD pattern of 0.01 wt% Si steel.

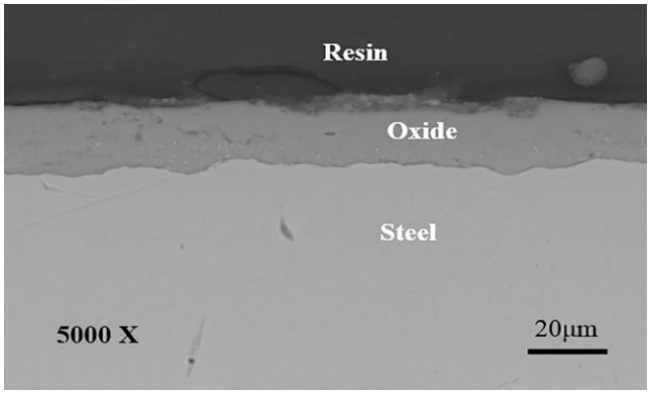

Figure 6. SEM image of 0.12 wt% Si steel.

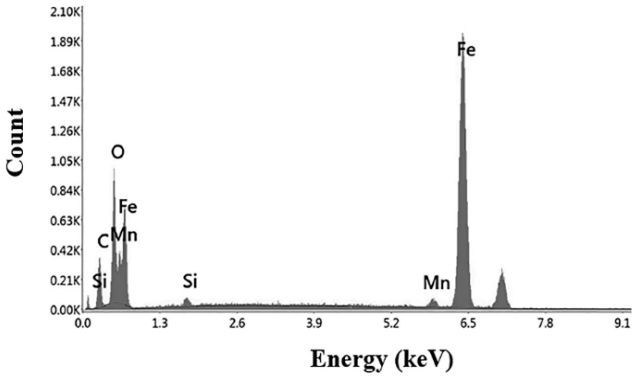

Figure 7. EDS pattern at steel-scale interface of 0.12 wt% Si steel.

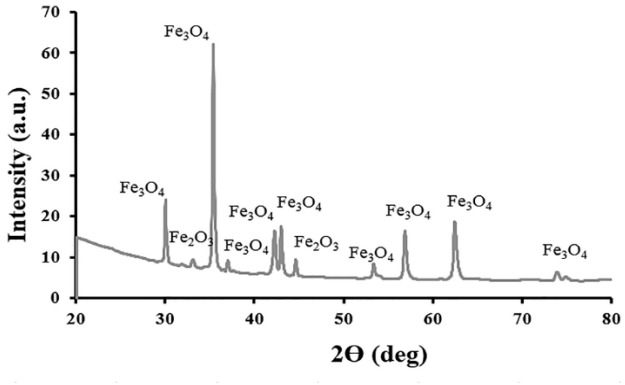

Figure 8. XRD pattern of 0.12 wt% Si steel.

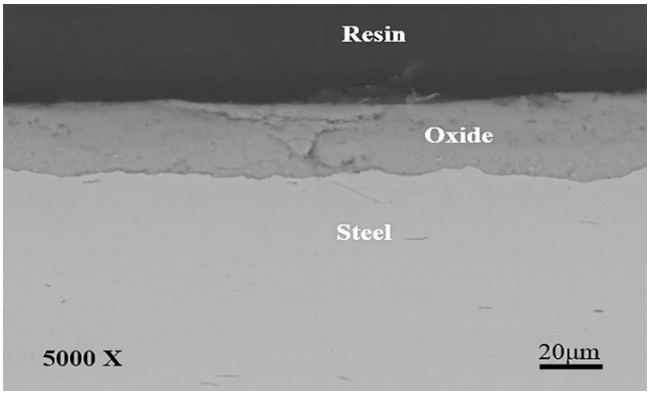

Figure 9. SEM image of 0.18 wt% Si steel.

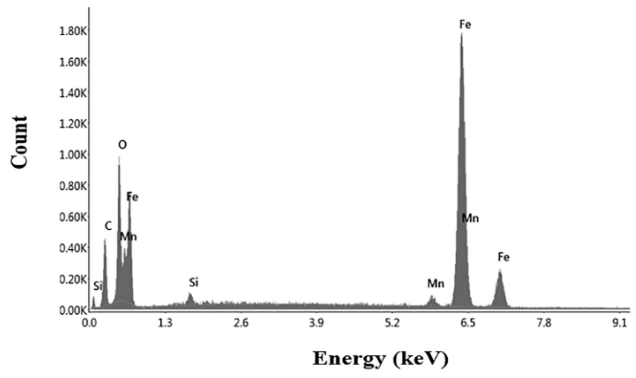

Figure 10. EDS pattern at steel-scale interface of 0.18 wt% Si steel.

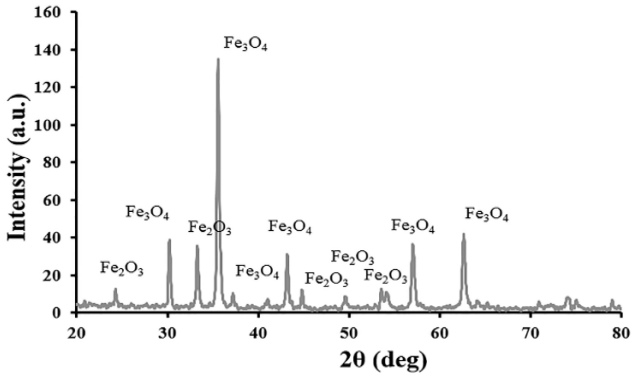

Figure 11. XRD pattern of 0.18 wt% Si steel.

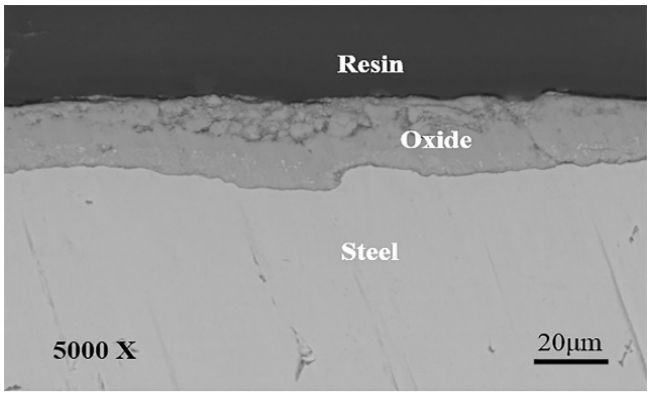

Figure 12. SEM image of 0.29 wt% Si steel.

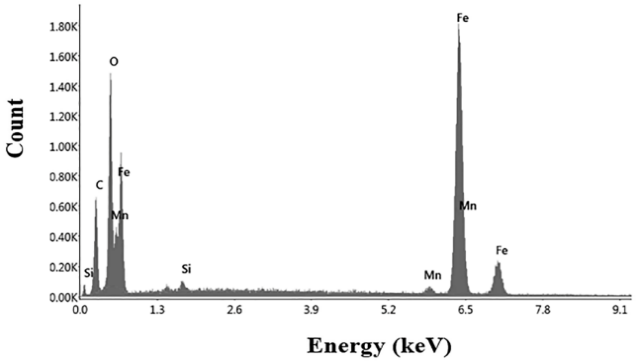

Figure 13. EDS pattern at steel-scale interface of 0.29 wt% Si steel.

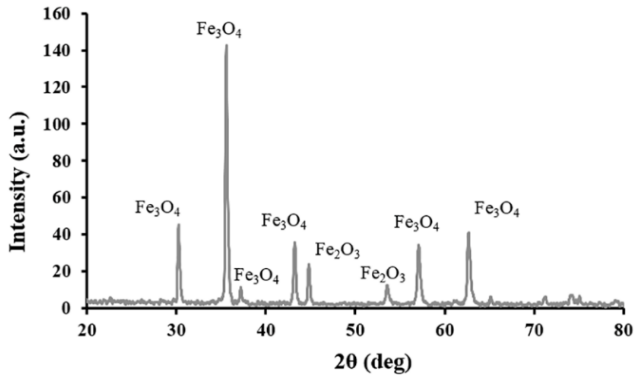

Figure 14. XRD pattern of 0.29 wt% Si steel.

3.2 Oxide scale adhesion

After tensile test, the scale adhesion can be described by the strain at the first spallation of scale. The oxide scale was spalled out of the steel substrate under tension loading. During the tensile test, stress was applied to the specimen until the stress exceeded the adhesive force between the scale and steel substrate. As a result, the oxide scale can be spalled. This was an important parameter for comparing the adhesion of hot-rolled steel with different silicon content. If the adhesion of scale was lower, the strain initiation of the first spallation was rapidly observed. Figure 15 shows strain initiating the first spallation of the Si-containing hot-rolled steel. It was found that the strain initiation the first spallation tended to increase with increasing silicon alloying content. However, the strain initiation the first spallation was decreased for 0.29 wt% Si steel. The strain initiation the first spallation of 0.01 wt% Si steel was 3.00 ± 0.45 %, for 0.12 wt% Si steel was 5.02 ± 0.59 %, for 0.18 wt% Si steel was 5.23 ± 0.20 %, and for 0.29 wt% Si steel was 4.68 ± 0.37 %. This variable can be used to calculate the mechanical adhesion energy of the scale on steel substrate.

As the strain at the first spallation, the mechanical adhesion energy was calculated by using Equation (1) [34,35]. The mechanical adhesion energy equation consists of stored energy (W) and oxide scale thickness (§). The strain at the first spallation was an important parameter used for calculating stored energy in oxide scale until the first spallation. The stored energy of oxide scale in x and y directions was considered by equation $\int \sigma \cdot d\varepsilon$ (the area under the stress-strain curve). Before the tensile test, the oxide scale and the steel substrate were assumed to be completely adhered. The parameters for quantifying the stored energy as follow, Young's modulus of steel and oxide was 210 GPa, Poisson's ratio of steel and oxide was 0.3, the compressive residual stress of oxide was – 0.2 GPa, and the strain at limit of elasticity of oxide was 0.0015.

$$G_i = W \cdot \S \quad (1)$$

Where G_i = Mechanical adhesion energy ($J \cdot m^{-2}$)
W = Stored energy in oxide scale until the first spallation ($J \cdot m^{-3}$)
§ = Oxide scale thickness (m)

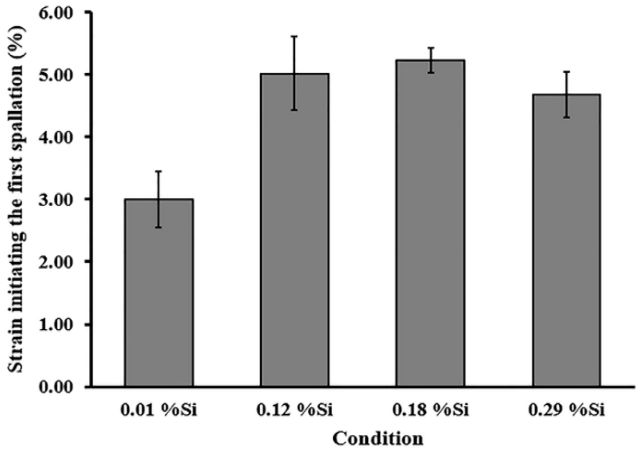

Figure 15. Strain initiating the first spallation of the Si-containing hot-rolled steel.

Table 2. Information about the Si-containing hot-rolled steel.

Parameters	Composition (wt% Si)			
	0.01	**0.12**	**0.18**	**0.29**
Scale thickness (μm)	11.30 ± 0.68	10.47 ± 0.43	10.05 ± 0.79	9.53 ± 0.46
Strain initiating the first spallation (%)	3.00 ± 0.45	5.02 ± 0.59	5.23 ± 0.20	4.68 ± 0.37
Mechanical adhesion energy ($J{\cdot}m^{-2}$)	335.32 ± 0.31	902.19 ± 0.36	941.92 ± 0.11	711.01 ± 0.14
Scale thickness (μm)	11.30 ± 0.68	10.47 ± 0.43	10.05 ± 0.79	9.53 ± 0.46

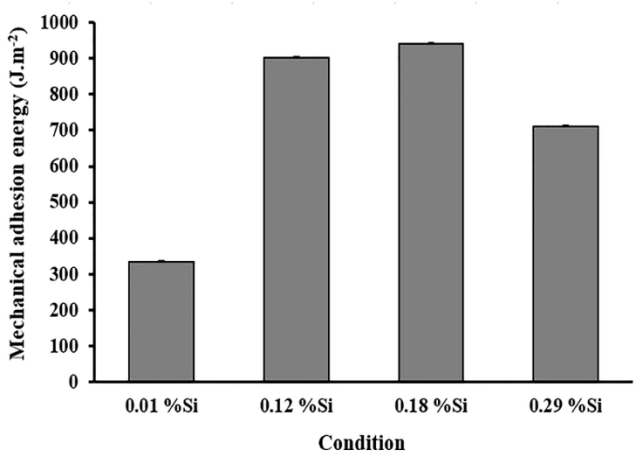

Figure 16. Mechanical adhesion energy of the Si-containing hot-rolled steel.

From there parameters, the calculated mechanical adhesion energy of the Si-containing hot-rolled steel was shown in Figure 16 with information in Table 2. It was found that the mechanical adhesion energy tends to increase with increasing silicon content, while decreasing at 0.29 wt% Si hot-rolled steel. The mechanical adhesion energy of 0.01 wt% Si steel was 335.32 ± 0.31 $J{\cdot}m^{-2}$, for 0.12 wt% Si steel was 902.19 ± 0.36 $J{\cdot}m^{-2}$, for 0.18 wt% Si steel was 941.92 ± 0.11 $J{\cdot}m^{-2}$, and for 0.29 wt% Si steel was 711.01 ± 0.14 $J{\cdot}m^{-2}$. From SEM-EDS results, an energy dispersive spectroscopy (EDS) was focused on steel-scale interface of their Si-containing steel. The EDS spectrum shows the peaks of C, Mn, Fe, O as well as Si for 0.12. 0.18, and 0.29 wt% Si steel. Furthermore, it was found that the higher amount of Si presented at the steel-scale interface was 0.29 wt% Si steel. Since Si was most easily oxidized, silicon oxide (SiO_2) was first formed at the steel-scale interface. According to literature [25], it was reported that the silicon oxide improves scale adhesion on steel substrate. However, that research studied steel with 0.026 wt% and 0.193 wt% Si. The result shows the 0.193 wt% Si steel exhibited higher scale adhesion than the 0.026 wt% Si steel.

If silicon oxide forms a thick layer in the case of 0.29 wt% Si in this study. It may result in a decrease in scale adhesion. The compressive stress was increased by the thicker SiO_2 layer formed at the steel-scale interface of the 0.29 wt% Si during thermal oxidation in the hot-rolling process. For this reason, it was a matter of discussion as the scale formed on 0.29 wt% Si steel showed a slight decrease in adhesion to the steel substrate.

4. Conclusions

The adhesion behavior of the scale formed on hot-rolled steel with different silicon content by using a tensile test was studied. The iron oxide scale thickness tends to decrease with increasing silicon content due to the protective layer SiO_2. The oxide scale was composed of hematite and magnetite. The mechanical adhesion energy of the oxide scale actually formed on Si-containing hot-rolled steel was shown to be in the range of 335 $J{\cdot}m^{-2}$ to 942 $J{\cdot}m^{-2}$. The high silicon content in hot-rolled steel tends to increase scale adhesion. Silicon should be added as low as possible for easy removal of scale in the de-scaling process for the hot-rolled steel industry.

Acknowledgements

This research was funded by National Science, Research and Innovation Fund (NSRF), and King Mongkut's University of Technology North Bangkok with Contract no. KMUTNB-FF-65-09. Hot-rolled steel was received from Sahaviriya Steel Industries Public Company Limited.

References

[1] X. J. Liu, Y. Q. He, G. M. Cao, T. Jia, T. Z. Wu, and Z. Y. Liu, "Effect of Si content and temperature on oxidation resistance of Fe-Si alloys," *Journal of Iron and Steel Research International,* vol. 22, no. 3, pp. 238-244, 2015.

[2] J. Eklund, B. Jönsson, A. Persdotter, J. Liske, J. E. Svensson, and T. Jonsson,"The influence of silicon on the corrosion properties of FeCrAl model alloys in oxidizing environments at 600°C," *Corrosion Science,* vol. 144, pp. 266-276, 2018.

[3] Y. L. Yang, C. H. Yang, S. N. Lin, C. H. Chen, and W. T. Tsai, "Effects of Si and its content on the scale formation on hot-rolled steel strips," *Materials Chemistry and Physics,* vol. 112, no. 2, pp. 566-571, 2008.

[4] D. Genève, D. Rouxel, P. Pigeat, and M. Confente, "Descaling ability of low-alloy steel wires depending on composition and rolling process." *Corrosion Science,* vol. 52, no. 4, pp. 1155-1166, 2010.

[5] Q. Yuan, G. Xu, M. X. Zhou, and B. He, "New insights into the effects of silicon content on the oxidation process in silicon-containing steels," *International Journal of Minerals, Metallurgy, and Materials,* vol. 23, no. 9, pp. 1048-1055, 2016.

[6] L. Suárez, P. Rodríguez-Calvillo, Y. Houbaert, and R. Colás, "Oxidation of ultra low carbon and silicon bearing steels," *Corrosion Science,* vol. 52, no. 6, pp. 2044-2049, 2010.

[7] H. Utsunomiya, K. Hara, R. Matsumoto, and A. Azushima, "Formation mechanism of surface scale defects in hot rolling process," *CIRP Annals,* vol. 63, no. 1, pp. 261-264, 2014.

[8] M. Z. G. Shao, "Characterization and properties of oxide scales on hot-rolled strips," *Materials Science and Engineering A,* vol. 452-453, pp. 189-193, 2007.

[9] R. Y. Chen, and W. Y. D. Yuen, "Oxidation of low-carbon, low-silicon mild steel at 450-900°C under conditions relevant to hot-strip processing," *Oxidation of Metals*, vol. 57, no.1/2, pp. 53-79, 2002.

[10] S. Liu, D. Tang, H. Wu, and L. Wang, "Oxide scales characterization of micro-alloyed steel at high temperature," *Journal of Materials Processing Technology,* vol. 213, no. 7, pp. 1068-1075, 2013.

[11] R. Y. Chen, and W. Y. D. Yuen, "Examination of oxide scales of hot rolled steel products," *Iron and Steel Institute of Japan International*, vol. 45, 1, pp. 52-59, 2005.

[12] P. Sarrazin, A. Galerie, and J. Fouletier, *Mechanisms of high temperature corrosion: a kinetic approach.* Materials Science Foundations, Trans Tech Publications, Stafa-Zürich, Switzerland, 2008.

[13] M. J. L. Gines, G. J. Benitez, T. Perez, E. Merli, M. A. Firpo, and W. Egli, "Study of the picklability of 1.8 mm hot-rolled steel strip in hydrochloric acid," *Latin American Applied Research*, vol. 32, pp. 281-288, 2002.

[14] Z. Y. Jiang, A. K. Tieu, W. H. Sun, J. N. Tang, and D. B. Wei, "Characterisation of thin oxide scale and its surface roughness in hot metal rolling," *Materials Science and Engineering A*, vol. 435-436, pp. 434-438, 2006.

[15] L. Suárez, R. Petrov, L. Kestens, M. Lamberigts, and Y. Houbaert, "Texture evolution of tertiary oxide scale during steel plate finishing hot rolling simulation tests," *Materials Science Forum*, vol. 550, pp. 557-562, 2007.

[16] S. Chandra-ambhorn, and K. Ngamkham, "High temperature oxidation of micro-alloyed steel and its scale adhesion," *Oxidation of Metals*, vol. 88, pp. 291-300, 2017.

[17] S. Chandra-ambhorn, T. Phadungwong, and K. Sirivedin, "Effects of carbon and coiling temperature on the adhesion of thermal oxide scales to hot-rolled carbon steels," *Corrosion Science*, vol. 115, pp. 30-40, 2017.

[18] S. Chandra-ambhorn, T. Nilsonthi, Y. Wouters, and A. Galerie, "Oxidation of simulated recycled steels with 0.23 and 1.03 wt% Si in Ar–20% H_2O at 900°C," *Corrosion Science*, vol. 87, pp. 101-110, 2014.

[19] S. Chandra-ambhorn, A. Jutilarptavorn, and T. Rojhirunsakool, "High temperature oxidation of irons without and with 0.06 wt% Sn in dry and humidified oxygen," *Corrosion Science*, vol. 148, pp. 355-365, 2019.

[20] S. Chandra-ambhorn, K. Ngamkham, and N. Jiratthanakul, "Effects of process parameters on mechanical adhesion of thermal oxide scales on hot-rolled low carbon steels," *Oxidation of Metals*, vol. 80, 1, pp. 61-72, 2013.

[21] Q. Yuan, G. Xu, M. Zhou, and B. He, "The effect of the Si content on the morphology and amount of Fe_2SiO_4 in low carbon steels," *Metals,* vol. 6, no. 4, pp. 94, 2016.

[22] Y. Yu, C. Wang, L. Wang, J. Chen, Y. J. Hui, and C. K. Sun, "Combination effect of Si and P on tertiary scale characteristic of hot rolled strip," *Journal of Iron and Steel Research International,* vol. 22, no. 3, pp. 232-237, 2015.

[23] A. Chattopadhyay, and T. Chanda, "Role of silicon on oxide morphology and pickling behaviour of automotive steels," *Scripta Materialia,* vol. 58, no. 10, pp. 882-885, 2008.

[24] M. Zhang, and G. Shao, "Characterization and properties of oxide scales on hot-rolled strips," *Materials Science and Engineering A*, vol. 452-453, pp. 189-193, 2007.

[25] T. Nilsonthi, J Tungtrongpairoj, S. Chandra-ambhorn, Y. Wouters, and A. Galerie, "Effect of silicon on formation and mechanical adhesion of thermal oxide scale grown on low carbon steels in a hot-rolling line," *Steel Research International,* pp. 987-990, 2012.

[26] T. Nishimoto, K. Honda, Y. Kondo, and K. Uemura, "Effects of Si content on the oxidation behavior of Fe-Si alloys in air," *Materials Science Forum*, vol. 696, pp. 126-131, 2011.

[27] E. Ahtoy, M. Picard, G. Leprince, A. Galerie, Y. Wouters, X. Wang, and A. Atkinson, "Time and temperature dependence of the adhesion of oxide scales formed on phosphorus-containing steels during short term oxidation," *Materials Chemistry and Physics,* vol. 148, no. 3, pp. 1157-1162, 2014.

[28] J. Liu, and G. Jiang, "Use of laboratory indentation tests to study the surface crack propagation caused by various indenters," *Engineering Fracture Mechanics,* vol. 241, pp. 407-421, 2021.

[29] M. M. Islam, S. I. Shakil, N. M. Shaheen, P. Bayati, and M. Haghshenas, "An overview of microscale indentation fatigue: Composites, thin films, coatings, and ceramics," *Micron,* vol. 148, pp. 103-110, 2021.

[30] K. Ngamkham, S. Niltawach, and S. Chandra-Ambhorn, "Development of tensile test to investigate mechanical adhesion of thermal oxide scales on hot-rolled steel strips produced using different finishing temperatures," *Key Engineering Materials,* vol. 462, pp. 407-412, 2011.

[31] G. Bamba, Y. Wouters, A. Galerie, F. Charlot, and A. Dellali, "Thermal oxidation kinetics and oxide scale adhesion of Fe–15Cr alloys as a function of their silicon content," *Acta Materialia,* vol. 54, no. 15, pp. 3917-3922, 2006.

[32] S. Vongsilathai, P. Thapanathitikul, K. Ngamkham, and T. Rojhirunsakool, "Effects of titanium and niobium on micro-structure and mechanical adhesion of thermal oxide scales on hot-rolled low carbon steel," *Suranaree Journal of Science & Technology,* vol. 26, no. 11, pp. 84-92, 2019.

[33] S. Chandra-Ambhorn, F. Roussel-Dherbey, F. Toscan, Y. Wouters, A. Galerie, and M. Dupeux, "Determination of mechanical adhesion energy of thermal oxide scales on AISI 430Ti alloy using tensile test," *Materials Science and Technology,* vol. 23, no. 4, pp. 497-501, 2007.

[34] H. E. Evans, "Stress effects in high temperature oxidation of metals," *International Materials Reviews,* vol. 40, no. 1, pp. 1-40, 1995.

[35] H. E. Evans, "Predicting oxide spallation from sulphur-contaminated oxide/metal interfaces," *Oxidation of Metals,* vol. 79, no. 1, pp. 3-14, 2013.